Random deposition with a power-law noise model: Multiaffine analysis

S. Hosseinabadi[1,*] and A. A. Masoudi[2,†]
[1]*Department of Physics, East Tehran Branch, Islamic Azad University, Tehran 18735-136, Iran*
[2]*Department of Physics, Alzahra University, Tehran 1993891167, Iran*

(Received 6 October 2018; published 17 January 2019)

We study the random deposition model with power-law distributed noise and rare-event dominated fluctuation. In this model instead of particles with unit sizes, rods with variable lengths are deposited onto the substrate. The length of each rod is chosen from a power-law distribution $P(l) \sim l^{-(\mu+1)}$, and the site at which each rod is deposited is chosen randomly. The results show that for $\mu < \mu_c = 3$ the log-log diagram of roughness, $W(t)$, versus deposition time, t, increases as a step function, where the roughness in each interval acts as $W_{\mathrm{loc}}(t) \approx t^{\beta_{\mathrm{loc}}}$. The local growth exponent, β_{loc}, is zero for $\mu = 1$. By increasing the μ exponent, the value of β_{loc} is increased. It tends to the growth exponent of the random distribution model with Gaussian noise, $\beta = 1/2$, at $\mu_c = 3$. The fractal analysis of the height fluctuations for this model was performed by multifractal detrended fluctuation analysis algorithm. The results show multiaffinity behavior for the height fluctuations at $\mu < \mu_c$ and the multiaffinity strength is greater for smaller values of the μ exponent.

DOI: 10.1103/PhysRevE.99.012130

I. INTRODUCTION

Recently there has been increasing attention to the study of morphology and dynamics of growing rough surfaces in the field of nonequilibrium statistical physics [1–3]. This interest is due to the challenge for the experimental physicist to shape rough surfaces with desired interfaces and for the theoretical physicist to model the geometrical and dynamical properties of interfaces during growth phenomena [4–6]. Exploring and modeling growth phenomena have considerable importance in the control of interfaces in industries and most research areas such as crystal growth [7,8], fluid flows [9], fire fronts [10], and biological and bacterial growth [11]. It has been observed that the mentioned interfaces and complex structures show some common features such as self-similarity or self-affinity that makes their study more easier [1–4].

To analyze the nonequilibrium growth phenomena one needs to combine insights from theoretical analysis and computational simulation to obtain favorite results. The fluctuations obtained during growth process are often characterized by statistical discrete models in which the complex interactions of atoms or molecules are replaced by simple deposition and relaxation rules implemented in kinetic Monte Carlo algorithms [12,13]. There are some statistical models that characterize many properties by ignoring the microscopic details of the rough surfaces during growth processes. Random deposition (RD) [14], random deposition with surface relaxation [15], ballistic deposition [16], Eden models [17], and solid-on-solid model [18,19] are examples of these statistical models that are useful for describing some properties of nonequilibrium growth phenomena.

The random deposition model is the simplest surface growth model, which has been discussed in various versions such as a random deposition-like model for two kinds of interacting particles [20], on-top site random-deposition model for epitaxial growth on a cubic substrate [21], random deposition for particles with different sizes [22], and multifractal scaling analysis of random deposition with varied sizes [23]. The differential equation that describes the variation of the height $h(x,t)$ with time t at any position x in the RD model is given by

$$\frac{\partial h(x,t)}{\partial t} = F + \eta(x,t), \tag{1}$$

where F is the average number of particles arriving at site x and $\eta(x,t)$ is a Gaussian distributed noise which denotes the random fluctuations in the deposition process. The value of $\eta(x,t)$ is chosen as an uncorrelated random number with zero average

$$\langle \eta(x,t) \rangle = 0 \tag{2}$$

without any correlation in space and time as

$$\langle \eta(x,t)\eta(x',t') \rangle = 2D\delta(x-x')(t-t'). \tag{3}$$

In this model the lateral correlations between depositing particles are completely inconsiderable.

In the most studies, it has been discussed how Gaussian and correlated noises can affect the roughness and dynamic exponents in discrete growth models [1,16–19]. On the other hand, there are events in which the amplitude of the noise changes as a power-law distribution. For example, such a power-law distributed noise has been observed in investigation of fluid flow in porous environments as well as the quenched noises resulting in evidence of a power-law distribution [1,24]. For

*shoseinabadi@iauet.ac.ir
†masoudi@alzahra.ac.ir

such a noise, the probability of an event of size η occurring is

$$P(\eta) \equiv \begin{cases} \mu\eta^{-(\mu+1)} & [\eta > 1] \\ 0 & [\eta < 1] \end{cases}, \tag{4}$$

where μ is an exponent which characterizes the decay of the noise amplitude. In the case of power-law noises, the events occur independently and are uncorrelated in space and time. In other words, very small and large events (rare events) in each site appear independently from the neighbors. In the case of Gaussian noises, the probability of the appearance of a rare event decreases exponentially with the size of that event. But for a power-law distributed noise, a decrease of this probability is much more slower than the exponential and the Gaussian ones. Therefore, the probability of evidence of a noise with very large amplitude is non-negligible. Furthermore, by decreasing the exponent μ the uniformity of the power-law noise is decreased. As μ increases the power-law noise approaches the Gaussian one, and the probability of appearing a large event becomes very small.

Every random process in nature generates fractal structures in which any irregularity could result in multifractal behavior [25–28]. A monofractal structure is uniform and free of irregularities and could be parameterized by a single scaling exponent in all scales, namely, the Hurst exponent H. The value of the Hurst exponent varies in the range of $0 < H < 1.0$. The value of $H = 0.5$ indicates a noncorrelated structure, while the exponents of $H < 0.5$ and $H > 0.5$ demonstrate anticorrelated and correlated systems, respectively. A rough surface with a greater value of the Hurst exponent seems locally smoother than the surface with a smaller one [25,26]. The concept of multiaffinity has provided deep insight into the complex nature of numerous important phenomena from the surface and interface sciences to cosmology [29–33]. The appearance of infinite different numbers of scaling exponents $h(q)$, where q is a real number, for a multifractal structure results in a much more appropriate description for it than the fractal dimension alone. In the multifractal structures, various regions of the system have different scaling features, and changing one of the $h(q)$ values could yield different properties of the system. It makes the theoretical and numerical investigation of multifractal structures more complicated than those of monofractal ones. Amitrano *et al.* [34] calculated the growth probability distribution in the kinetic aggregation process using the Green's function technique and investigated the multifractality behavior. Furthermore, the multifractal properties of diffusion-limited aggregation surfaces [35,36], the solid-on solid model [37], ballistic deposition with power-law noise [38], and the random-deposition model [23] have been investigated through multifractal scaling analysis.

The studies of the surfaces and the growth models obeying the Edward-Wilkinson and Kardar-Parizi-Zhang (KPZ) equations with Gaussian noise have presented a monofractal structure and a constant Hurst exponent [1]. Furthermore, Barabasi *et al.* [38] presented numerical evidence of multiaffine scaling for the KPZ model with power-law noise. Their calculations were based on the normalized qth-order correlation function of the height differences. On the other hand, Buldyrev *et al.* [39] investigated the ballistic deposition model with power-law noise and calculated the roughness and growth exponents via the Family-Vicsek scaling relation. Furthermore, they obtained the critical value $\mu_c = 5$ for the one-dimensional version of this model.

In this study, we have applied multifractal detrending fluctuation analysis (MF-DFA) to the growing surfaces of random deposition model with power-law distributed noise. We have studied in particular how the rare events appearance and the exponent of power noise decay, μ, could affect the growth exponent β and strength of multiaffinity. The paper is organized as follows. In Sec. II the method of generation of rough surfaces is presented, and Sec. III gives the details of the multifractal scaling analysis. In Sec. IV we present and discuss the results. Conclusions are given in Sec. V.

II. MODEL

In this study, the random deposition with power-law noise (RD-PLN) model is investigated. In the simple form of this model, particles fall down vertically onto a smooth surface. A site of the surface with linear size of L is randomly chosen, and then a particle falls in a straight-line trajectory and deposits onto the top of the column under it. Therefore, the height of the selected site, $h(x)$, is increased by one. There is no correlation between two neighboring sites in this model. Here we generate in $1 + 1$ dimensions the height fluctuation of $h(x, t)$ on a substrate with size L in different growth times t for the RD model with power-law chosen noise $\eta(x, t)$. Starting from a flat interface $h(x, t) = 0$ for all x at $t = 0$, the height growth proceeds up to time t, by the following rules:

(1) A position x is chosen randomly in the range of $[1, L]$ in which a rod will be deposited.

(2) The length of the rod is chosen as

$$l = \text{int}(r^{-\frac{1}{\mu}}), \tag{5}$$

where r is a random variable chosen uniformly in the range of (0,1) and the rod length l will be the largest integer number less than or equal to $r^{-\frac{1}{\mu}}$ [39].

(3) Finally the rod with the given length is deposited onto the chosen site, and the height is increases as

$$h(x, t + 1) = h(x, t) + l. \tag{6}$$

Each time step in our Monte Carlo simulation was considered equal to L so that exactly L rods are deposited in each time step. We carried out simulations for different values of parameters L, t, and μ.

The interface width or the rms roughness of the height fluctuations in different time steps of t was determined by the following relation:

$$W(L, t) \equiv \left\langle \left[\frac{1}{L} \sum_x [h(x, t) - \overline{h}(t)]^2 \right]^{1/2} \right\rangle, \tag{7}$$

where $\overline{h}(t)$ is the spatial average of height at time t. In short times, the interface width increases as a power of time:

$$W(L, t) \approx t^{\beta}. \tag{8}$$

Here the exponent β is called the growth exponent and characterizes the time-dependent dynamical behavior of the

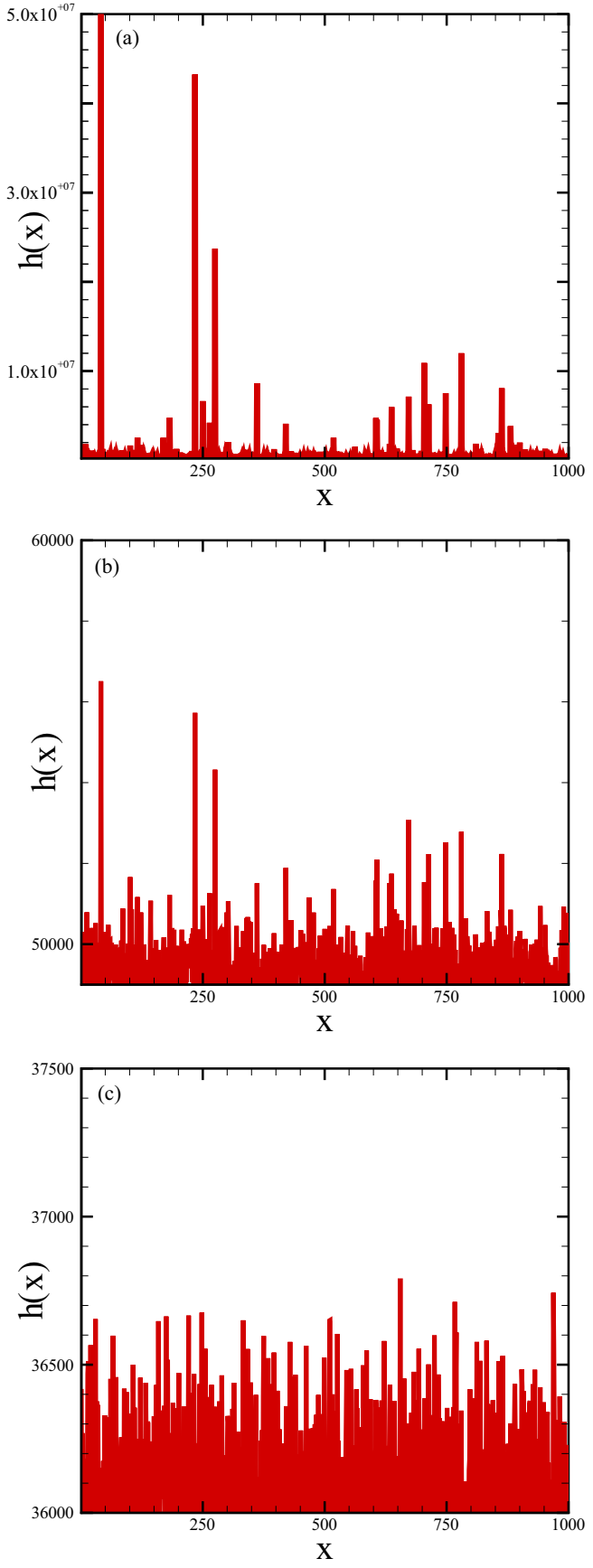

FIG. 1. The height profile obtained for different exponents of μ at the time step $t = 3000$. (a) $\mu = 1$, (b) $\mu = 2$, and (c) $\mu = 3$.

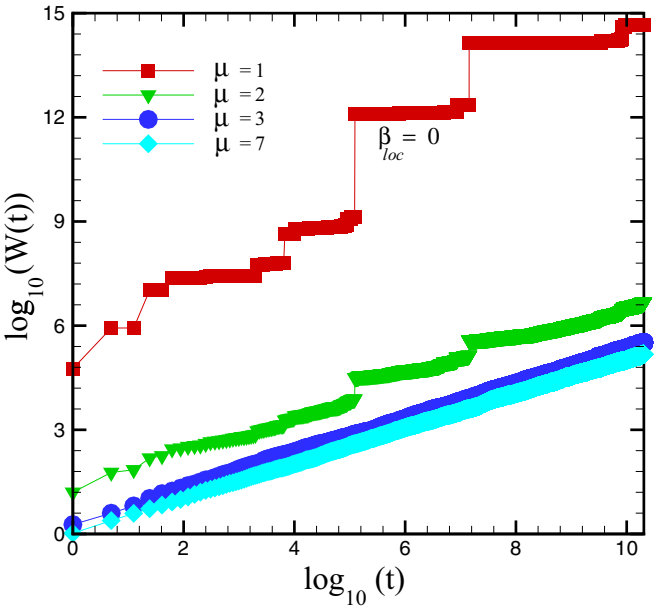

FIG. 2. Log-log diagram of roughness, $W(t)$, versus deposition time, t. For $\mu < \mu_c = 3$, $W(t)$ is increased as a step function where in each interval, $W_{\rm loc}(t) \approx t^{\beta_{\rm loc}}$. The exponent $\beta_{\rm loc} = 0$, for $\mu = 1$. Increasing the μ exponent leads to enhancement of $\beta_{\rm loc}$ so that for $\mu \geqslant \mu_c = 3$, $\beta_{\rm loc} \to \beta = 1/2$.

growth process. The exact value of $\beta = \frac{1}{2}$ has been obtained analytically and numerically for the random deposition model with Gaussian noise distribution. Now in this study it has been investigated how the rare events due to the power-law distributed noise could affect the roughness and growth exponent of the model.

III. MULTIFRACTALITY OF SYNTHETIC ROUGH SURFACE

There are various methods to distinguish the multiaffinity in complex structures such as spectral analysis [40], fluctuation analysis [41], detrended fluctuation analysis (DFA) [42,43], and wavelet transform module maxima [44,45]. However, in the case of noisy data, it has been shown that the MF-DFA algorithm despite a bit more effort in programming gives very reliable results [42]. The MF-DFA method has became a widely used technique for the determination of (multi-) fractal scaling properties in noisy, nonstationary time series [46,47]. It has successfully been applied to diverse fields such as DNA sequences [48], heart rate dynamics [49], cloud structure [50], solid state physics [51], sunspot time series [52], and experimental data from rough surfaces [53].

In this study, we rely on MF-DFA to characterize the height fluctuations generated during the RD growth model with power-law noise. In this method, we denote the height of the fluctuations by $\mathcal{H}(\mathbf{i})$. The MF-DFA in one dimension has the following steps [42]:

(1) Consider an array $\mathcal{H}(i)$ where $i = 1, 2, \ldots, M$. Divide the $\mathcal{H}(i)$ into M_s nonoverlapping segments of equal sizes s, where $M_s = [\frac{M}{s}]$. Each segment can be denoted by $\mathcal{H}_\nu$ such

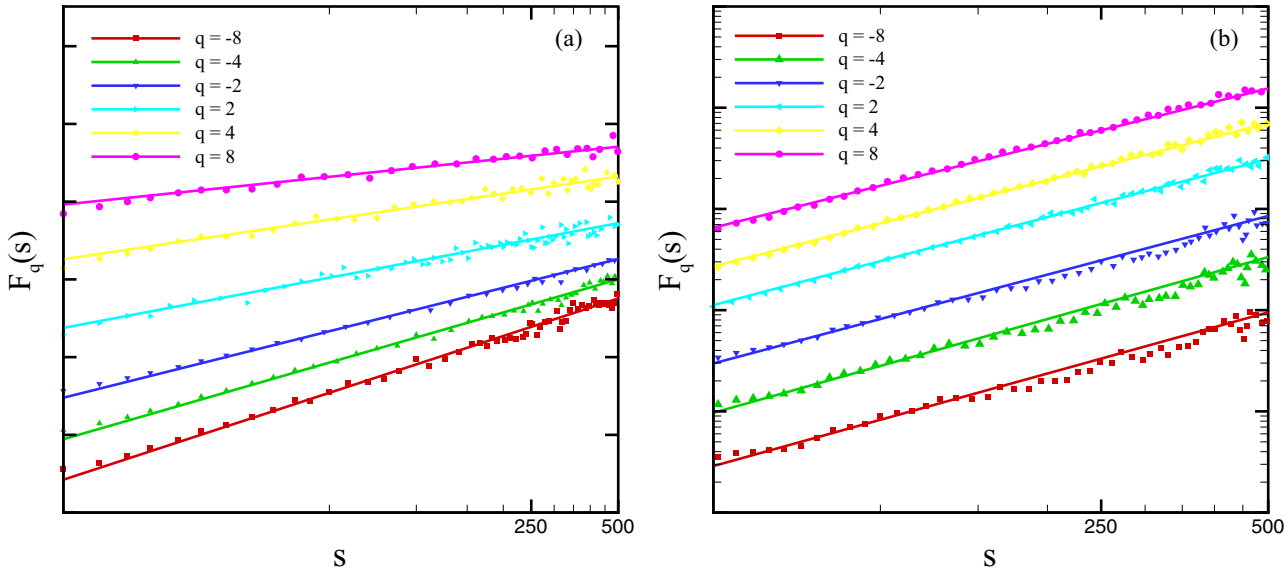

FIG. 3. The qth-order fluctuation function, $F_q(s)$, with respect to segment size, s, for different values of q and the exponents of $\mu = 1$ (a) and $\mu = 3$ (b). We shifted the y axis vertically.

that $\mathcal{H}_\nu(i) = \mathcal{H}(n+i)$ for $1 \leqslant i \leqslant s$, where $n = (\nu - 1)s$ and $\nu = 1, \ldots, M_s$.

(2) For each nonoverlapping segment, the cumulative sum is calculated by

$$Y_\nu(i) = \sum_{k=1}^{i} \mathcal{H}_\nu(k), \tag{9}$$

where $1 \leqslant i \leqslant s$.

(3) Calculate the local trend for each segment by a least-square fit of the profile:

$$\mathcal{B}_\nu(i) = ai + b. \tag{10}$$

Then determine the variance for each segment as follows:

$$\mathcal{D}_\nu(i) = Y_\nu(i) - \mathcal{B}_\nu(i), \tag{11}$$

$$F_\nu^2(s) = \frac{1}{s} \sum_{i=1}^{s} \mathcal{D}_\nu^2(i). \tag{12}$$

(4) Average over all segments to obtain the qth-order fluctuation function

$$F_q(s) = \left\{ \frac{1}{2M_s} \sum_{\nu=1}^{2M_s} \left[F_\nu^2(s) \right]^{q/2} \right\}^{1/q}, \tag{13}$$

where $F_q(s)$ depends on scale s for different values of q. It is easy to see that $F_q(s)$ increases with increasing s. Notice that $F_q(s)$ depends on the order q. In principle, q can take any real value except zero. For $q = 0$, Eq. (13) becomes

$$F_0(s) = \exp\left[\frac{1}{4M_s} \sum_{\nu=1}^{2M_s} \ln F_\nu^2(s) \right]. \tag{14}$$

For $q = 2$ the standard DFA in one dimension will be retrieved.

(5) Finally, determine the scaling behavior of the fluctuation functions by analyzing log-log plots of $F_q(s)$ versus s for each value of q:

$$F_q(s) \sim s^{h(q)} \tag{15}$$

It has been shown that for FBM nonstationary signals, the Hurst exponent is given by

$$H \equiv h(q = 2) - 1. \tag{16}$$

Using standard multifractal formalism [42] we have

$$\tau(q) = qh(q) - 1. \tag{17}$$

The singularity spectrum, $f(\alpha)$, of a multifractal rough surface is given by the Legendre transformation of $\tau(q)$ as [54]

$$f(\alpha) = q\alpha - \tau(q), \tag{18}$$

where $\alpha = \frac{\partial \tau(q)}{\partial q}$. It is well known that for a multifractal surface, various parts of the feature are characterized by different values of α causing a set of Hölder exponents instead of a single α. The interval of a Hölder spectrum, $\alpha \in [\alpha_{\min}, \alpha_{\max}]$, can be determined by [54]

$$\alpha_{\min} = \lim_{q \to +\infty} \frac{\partial \tau(q)}{\partial q}, \tag{19}$$

$$\alpha_{\max} = \lim_{q \to -\infty} \frac{\partial \tau(q)}{\partial q}. \tag{20}$$

IV. RESULTS AND DISCUSSION

In this study, the RD-PLN model, as discussed in Sec. II, was simulated, and the height fluctuations obtained for different exponents μ have been demonstrated in Fig. 1. As this figure shows the rare events are dominant at smaller values of μ exponents. At the value of $\mu = \mu_c = 3$, the height fluctuation is the same as the height in the simple RD model with a Gaussian noise distribution. The interface width in

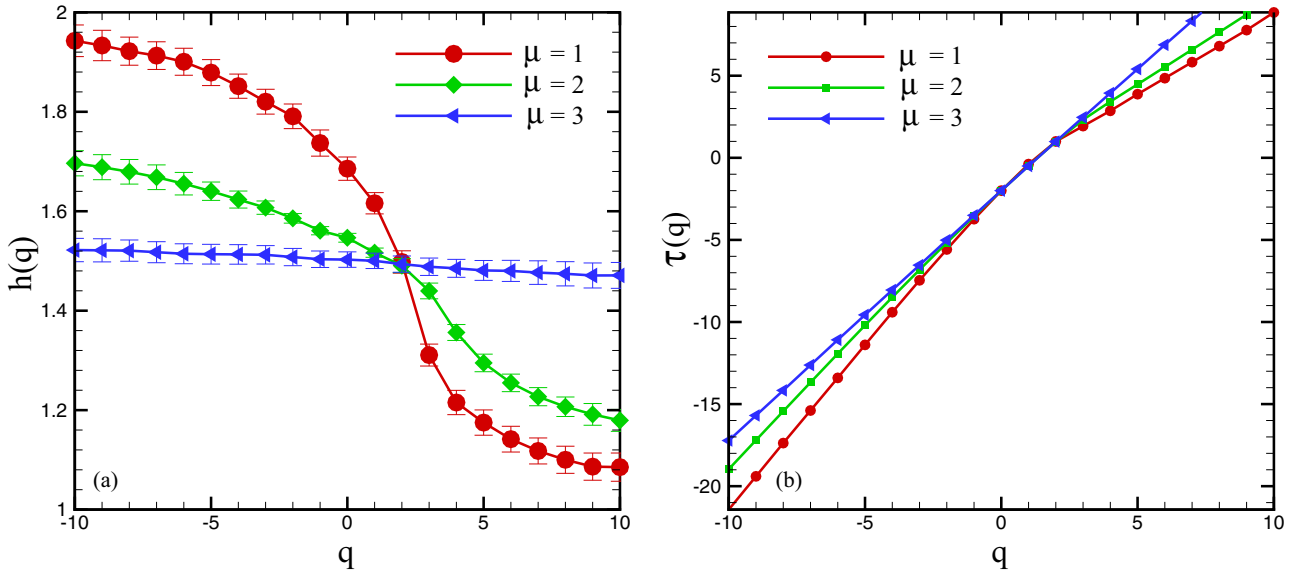

FIG. 4. The $h(q)$ and $\tau(q)$ spectra calculated from the scaling relation (15) and Eq. (17) for different values of μ exponents.

different time steps was determined via the relation (7). The log-log diagram of $W(t)$ versus t has been illustrated in Fig. 2. Because of existence of big jumps in the height fluctuations for small μ, the interface width does not increase continuously as seen in large values of μ. This figure represents that for $\mu < \mu_c = 3$ the logarithmic diagram of roughness versus time increases as a step function where in each interval $W_{\rm loc}(t) \approx t^{\beta_{\rm loc}}$. The local growth exponent is $\beta_{\rm loc}$ for $\mu = 1$. By increasing the μ exponent, the value of $\beta_{\rm loc}$ is increased. It tends to the the growth exponent of the simple RD model with Gaussian noise, $\beta = 1/2$, at $\mu_c = 3$. It is notable that we simulated our model for different system sizes, L. Figure 2 shows the results for $L = 1000$. The results demonstrated that the values of $\beta_{\rm loc}$ and $\beta = 1/2$ were independent of the system size. The independence of $\beta = 1/2$ from the system size for a simple RD model has been discussed in Ref. [1]. The fractal analysis of the height fluctuations in this model was performed by the MF-DFA algorithm as discussed in Sec. III. Figure 3 represents the qth-order fluctuation function, $F_q(s)$, with respect to segment size, s, for different values of q and the exponents of $\mu = 1$ and $\mu = 3$. One can see that for $\mu = 1$, the slopes of the curves for different q are varied, while the same diagram for $\mu = 3$ represents the same slopes for various q. Therefore, the height fluctuation generated via the exponent $\mu = 1$ in the RD-PLN model, has a multiaffine behavior. The $h(q)$ spectrum calculated from the scaling

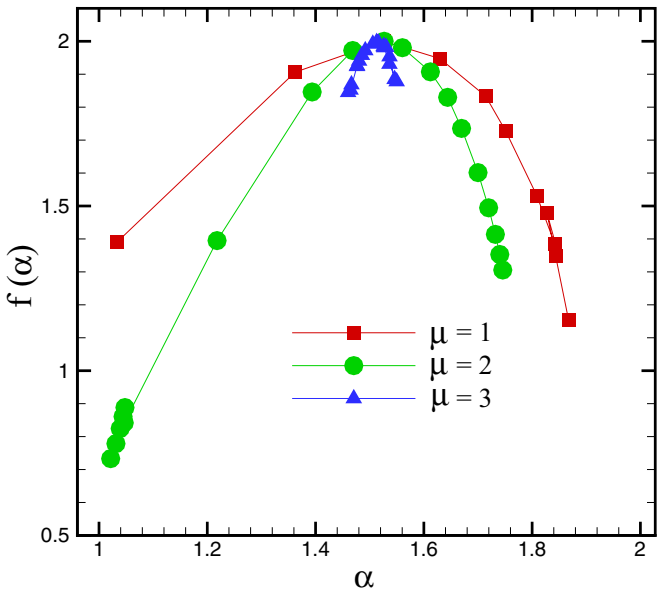

FIG. 5. The multiaffinity strength determined via the relation (18) for the height fluctuations with different μ exponents.

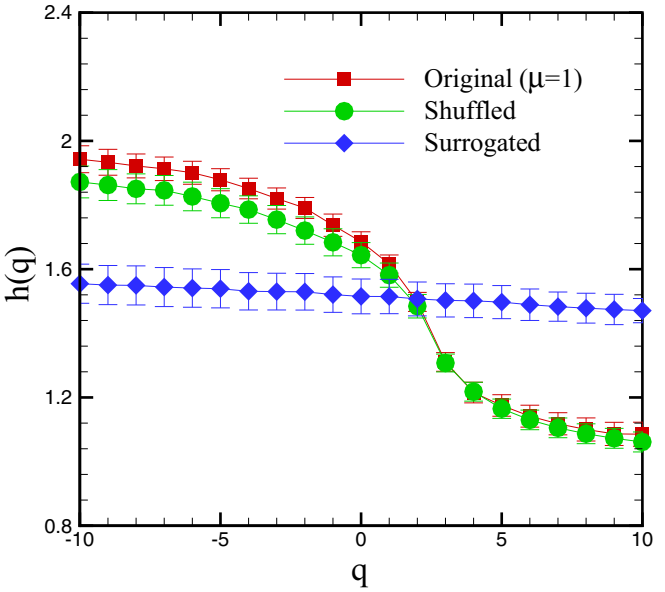

FIG. 6. The $h(q)$ spectrum for the shuffled and surrogate data of the height fluctuations with $\mu = 1$.

relation (15) has been illustrated in Fig. 4 for different values of the μ exponents. As this figure shows, by enhancement of μ exponent, the nonlinearity of the curves is decreased and tends to a straight line with the same $h(q) = H = 1/2$ in the case of $\mu = \mu_c = 3$. The multiaffinity strength was determined via the relation (18) for the height fluctuations with different μ exponents. Figure 5 shows that the multiaffinity strength is greater for smaller values of μ exponent. Regarding the source of multiaffinity, it is notable that the quenched noises, power-law distribution noises, and surface diffusion in some simple models could result in multiaffine interfaces [1]. Furthermore, in general two kinds of multiaffinity could be distinguished as [33,55] the broadness of the probability density function of the height fluctuations and different long-range correlations for small and large fluctuations. In this study, the power-law noise and the deviation of the height fluctuations distribution from the normal one could be the reason of multiaffinity behavior. To show this claim, the $h(q)$ spectrum for the shuffled and surrogate data of the height fluctuations with $\mu = 1$ was considered [33]. The shuffling of the data does not change the power-law distribution, and the $h(q)$ spectrum remains a nonlinear function of the q value in Fig. 6. As this figure shows, the surrogate height fluctuations with a Gaussian distribution have a nondependent $h(q)$ spectrum.

V. CONCLUSIONS

We studied the random deposition model with power-law distributed noise. In this model the rods with variable lengths are deposited onto the substrate instead of particles with unit sizes. The length of each rod is chosen from a power-law distribution, $P(l) \sim l^{-(\mu+1)}$, and the site at which the rods are deposited is chosen randomly. The results show that for $\mu < \mu_c = 3$ the log-log diagram of roughness, $W(t)$, versus deposition time, t, increased as a step function, where the roughness in each interval acts as $W_{\rm loc}(t) \approx t^{\beta_{\rm loc}}$. for $\mu = 1$ the local growth exponent, $\beta_{\rm loc}$, is equal to 0. By increasing the μ exponent, the value of $\beta_{\rm loc}$ is increased. It tends to the growth exponent of the RD model with Gaussian noise, $\beta = 1/2$, at $\mu_c = 3$. The fractal analysis of the height fluctuations in this model was performed by multifractal detrended fluctuation analysis (MF-DFA) algorithm. The results show multiaffinity behavior for the height fluctuations with $\mu < \mu_c$ and the multiaffinity strength is greater for smaller values of the μ exponent.

ACKNOWLEDGMENTS

The work of S.H. was supported by Islamic Azad University, East Tehran Branch. The work of A.A.M. was supported by the research council of Alzahra University (Tehran, Iran).

[1] A. L. Barabasi and H. E. Stanly, *Fractal Concepts in Surface Growth* (Cambridge University Press, New York, 1995).
[2] J. Feder, *Fractals* (Plenum Press, New York, 1988).
[3] F. Family and T. Viscek, *Dynamics of Fractal Surfaces* (World Scientific, Singapore, 1990).
[4] C. B. Duke and E. W. Plummer (eds.), *Frontiers in Surface and Interface Science* (Elsevier, Amsterdam, 2002).
[5] A. Kolakowska, M. A. Novotny, and P. S. Verma, Phys. Rev. E **73**, 011603 (2006).
[6] F. D. A. A. Reis, Phys. Rev. E **69**, 021610 (2004).
[7] B. Sapoval, J. Gouyet, M. Rosso, A. Bunde, and S. Havlin (eds.), *Fractals and Disordered Systems* (Springer-Verlag, Berlin, 1991).
[8] A. Pimpinelli and J. Villain, *Physics of Crystal Growth* (Cambridge University Press, Cambridge, 1999).
[9] T. H. Kwon, A. E. Hopkins, and S. E. O'Donnell, Phys. Rev. E **54**, 685 (1996).
[10] J. Zhang, Y.-C. Zhang, P. Alstrom, and M. Levinsen, Physica A: Stat. Mech. Appl. **189**, 383 (1992).
[11] A. Epstein, A. Hochbaum, P. Kim, and J. Aizenberg, Nanotechnology **22**, 49 (2011).
[12] T. Shitara, D. D. Vvedensky, M. R. Wilby, J. Zhang, J. H. Neave, and B. A. Joyce, Phys. Rev. B **46**, 6815 (1992).
[13] J. W. Evans, P. A. Thiel, and M. C. Bartelt, Surf. Sci. Rep. **61**, 1 (2006).
[14] F. Family, J. Phys. A **19**, L441 (1986).
[15] R. C. Buceta, D. Hansmann, and B. von Haeften, J. Stat. Mech.: Theory Exp. (2014) P12028.
[16] P. Meakin, P. Ramanlal, L. M. Sander, and R. C. Ball, Phys. Rev. A **34**, 5091 (1986).
[17] R. Jullien and R. Botet, J. Phys. A **18**, 2279 (1985).
[18] J. M. Kim and J. M. Kosterlitz, Phys. Rev. Lett. **62**, 2289 (1989).
[19] S. Hosseinabadi, A. A. Masoudi, and M. Sadegh Movahed, Physica B **405**, 2072 (2010).
[20] H. F. El-Nashar and H. A. Cerdeira, Sur. Sci. **415**, 1 (1998).
[21] J. W. Evans, Phys. Rev. B **39**, 5655 (1989).
[22] F. L. Forgerini and W. Figueiredo, Phys. Rev. E **79**, 041602 (2009).
[23] A. Chaudhari, C.-C. S. Yan, and S.-L. Lee, Appl. Surf. Sci. **238**, 513 (2004).
[24] Y.-C. Zhang, Physica A **170**, 1 (1990).
[25] D. Sornette, *Critical Phenomena in Natural Sciences: Chaos, Fractals, Self-organization and Disorder: Concepts and Tools* (Springer-Verlag, Heidelberg, 2000).
[26] H. E. Stanley and P. Meakin, Nature (London) **335**, 405 (1988).
[27] S. Hosseinabadi, M. A. Rajabpour, M. Sadegh Movahed, and S. M. Vaez Allaei, Phys. Rev. E **85**, 031113 (2012).
[28] S. Hosseinabadi and M. Rajabi, Superlattices Microstruct. **102**, 180 (2017).
[29] A. Chaudhari, G. Rabbani, and S.-L. Lee, J. Chin. Chem. Soc. **54**, 1201 (2007).
[30] P. K. Mandal and D. Jana, Phys. Rev. E **77**, 061604 (2008).
[31] M. Vahabi, G. R. Jafari, N. Mansour, R. Karimzadeh, and J. Zamiranvari, J. Stat. Mech.: Theory Exp. (2008) P03002.
[32] S. Hosseinabadi, A. Mortezaali, and A. A. Masoudi, Surf. Interface Anal. **40**, 71 (2008).
[33] M. S. Movahed, F. Ghasemi, S. Rahvar, and M. R. Tabar, Phys. Rev. E **84**, 021103 (2011).
[34] C. Amitrano, A. Coniglio, and F. di Liberto, Phys. Rev. Lett. **57**, 1016 (1986).
[35] J. Nittmann, H. E. Stanley, E. Touboul, and G. Daccord, Phys. Rev. Lett. **58**, 619 (1987).

[36] W. G. Hanan and D. M. Heffernan, Phys. Rev. E **85**, 021407 (2012).
[37] W. Bing, W. Yan, and W. Ziqin, Solid State Commun. **96**, 69 (1995).
[38] A.-L. Barabási, R. Bourbonnais, M. Jensen, J. Kertész, T. Vicsek, and Y.-C. Zhang, Phys. Rev. A **45**, R6951(R) (1992).
[39] S. V. Buldyrev, S. Havlin, J. Kertész, H. E. Stanley, and T. Vicsek, Phys. Rev. A **43**, 7113(R) (1991).
[40] H. E. Hurst, Trans. Am. Soc. Civ. Eng. **116**, 770 (1951).
[41] C. K. Peng, S. Buldyrev, A. Goldberger, S. Havlin, F. Sciortino, M. Simons, and H. E. Stanley, Nature (London) **356**, 168 (1992).
[42] J. W. Kantelhardt, S. A. Zschiegner, E. Koscielny-Bunde, S. Havlin, A. Bunde, and H. E. Stanley, Physica A **316**, 87 (2002).
[43] K. Hu, P. Ch. Ivanov, Z. Chen, P. Carpena, and H. E. Stanley, Phys. Rev. E **64**, 011114 (2001).
[44] Z. R. Struzik, and A. P. J. M. Siebes, Physica A **309**, 388 (2002).
[45] J. Arrault, A. Arneodo, A. Davis, and A. Marshak, Phys. Rev. Lett. **79**, 75 (1997).
[46] J. W. Kantelhardt, E. Koscielny-Bunde, H. A. Rego, S. Havlin, and A. Bunde, Physica A **295**, 441 (2001).
[47] Z. Chen, P. Ch. Ivanov, K. Hu, and H. E. Stanley, Phys. Rev. E **65**, 041107 (2002).
[48] S. V. Buldyrev, N. V. Dokholyan, A. L. Goldberger, S. Havlin, C. K. Peng, H. E. Stanley, and G. M. Viswanathan, Physica A **249**, 430 (1998).
[49] A. Bunde, S. Havlin, J. W. Kantelhardt, T. Penzel, J. H. Peter, and K. Voigt, Phys. Rev. Lett. **85**, 3736 (2000).
[50] K. Ivanova, M. Ausloos, E. Clothiaux, and T. P. Ackerman, Europhys. Lett. **52**, 40 (2000).
[51] N. Vandewalle, M. Ausloos, M. Houssa, P. W. Mertens, and M. Heyns, Appl. Phys. Lett. **74**, 1579 (1999).
[52] M. S. Movahed, G. R. Jafari, F. Ghasemi, S. Rahvar, and M. R. M. Tabar, J. Stat. Mech. (2006) P02003.
[53] S. Hosseinabadi, F. Abrinaei, and M. Shirazi, Physica A **481**, 11 (2017).
[54] A. Arneodo, E. Bacry, and J. F. Muzy, Physica A **213**, 232 (1994).
[55] A. Madanchi, M. Absalan, G. Lohmann, M. Anvari, and M. R. R. Tabar, Solar Energy **144**, 1 (2017).